AD-A250 221

REPORT DOCUMENTATION PAGE

Form Approved OMB No. 0704-0188

2

2. REPORT DATE

3. REPORT TYPE AND DATES COVERED
Final 15 May '89 - 14 Oct.'91

4. TITLE AND SUBTITLE
Turbulent Spot Generation and Growth Rates in a Transonic Boundary Layer

5. FUNDING NUMBERS
2307/DS
61102 F

6. AUTHOR(S)
J.P. Clark - Oxford University
J.E. LaGraff - Syracuse University
T.V. Jones - Oxford University

AFOSR-TR- 92 0365

7. PERFORMING ORGANIZATION NAME(S) AND ADDRESS(ES)
University of Oxford
Dept. Engineering Science
Parks Rd.
Oxford OX13PJ, UK

Syracuse University
Mechanical & Aerospace Eng
151 Link Hall
Syracuse, NY 13244

8. PERFORMING ORGANIZATION REPORT NUMBER
N.A.

9. SPONSORING/MONITORING AGENCY NAME(S) AND ADDRESS(ES)
AFOSR/NA
Bolling AFB, DC 20332-6448

10. SPONSORING/MONITORING AGENCY REPORT NUMBER
AFOSR-89-0427

11. SUPPLEMENTARY NOTES
Complete material to be published as Oxford University, D.Phil dissertation in late 1992 as submitted by J.P. Clark

12a. DISTRIBUTION/AVAILABILITY STATEMENT

Approved for public release; distribution unlimited

12b. DISTRIBUTION CODE

92-12945

13. ABSTRACT *(Maximum 200 words)*

Wide-bandwidth surface heat transfer instrumentation has been used to track the generation, convection and growth of turbulent spots in a laminar boundary layer undergoing transition to turbulence. The model was a flat plate subjected to a range of free stream conditions in a piston-driven isentropic compression heated transient wind tunnel at Oxford University. Freestream Mach number (subsonic to 2.0), freestream turbulence and streamwise pressure gradient (favorable to adverse) were varied. Preliminary analysis of the time-resolved heat transfer data allowed estimates of spot convection rates, generation rates and spreading angles to be estimated. Convection rates were little affected by Mach number whereas spreading angles were narrowed by favorable pressure gradients and expanded by adverse gradients.

14. SUBJECT TERMS
boundary layers, transition, turbulent spots, compressibility effects

15. NUMBER OF PAGES
23

16. PRICE CODE

17. SECURITY CLASSIFICATION OF REPORT	18. SECURITY CLASSIFICATION OF THIS PAGE	19. SECURITY CLASSIFICATION OF ABSTRACT	20. LIMITATION OF ABSTRACT
U	U	U	

Turbulent Spot Generation and Growth Rates in a Transonic Boundary Layer

Final Report to
United States Air Force Office of Scientific Research
Grant Number 89-0427

for period 15 May 1989-14 October 1991

J.P. Clark and Prof. T.V. Jones
Oxford University, Oxford, UK

Prof. J.E. LaGraff
Syracuse University, Syracuse, NY, USA

18 March 1992

FINAL TECHNICAL REPORT : AFOSR Grant No. 89-0427

Introduction

Preliminary results of the present experimental program performed under Grant No. 89-0427 were presented in Clark, et al. (Ref. 1 and attached as Appendix I). More recently, the experimental program has been completed, and data reduction methods have been developed to extract detailed turbulent-spot trajectory information. In this report, the analysis techniques are described and some of the most recently obtained results are presented. An abstract of a paper accepted for presentation at an AGARD conference in October, 1992 in Antalya, Turkey is attached as Appendix II. A complete treatment of the findings will be formed in the dissertation of J.P. Clark, to be published by Oxford University.

Analysis Techniques

The parameter which best describes the state of the boundary layer during transition is the intermittency. The variation of intermittency through the transition zone is dictated by the rates of turbulent-spot generation, convection, and lateral spreading. As it happens, the first two of these parameters could be determined from the results of a digital intermittency detector. The third was readily calculated through estimates of the rate of change of gauge coverage with distance along the flat-plate model surface.

Intermittency detectors, either analog or digital, have been known for a number of years. A comprehensive review of the detection technique was given by Hedley and Keffer (Ref. 2). In essence, a raw signal is transformed in such a way that a decision for or against the presence of turbulence at the sensor can be rationally made. Typically, the signal is differentiated and squared in order to emphasize its high frequency components. This, after Hedley and Keffer, is called the detector

function. Then, the signal is smoothed over a number of samples to create the criterion function. Finally, a threshold level is set and the intermittency signal determined.

The process by which turbulent/non-turbulent decisions were made in this case is illustrated in Figure 1. The top trace in Figure 1 is the unsteady-heat-transfer signal. The second trace from the top is the detector function, which in this case is defined as

$$D_i = m\, q_i'^{\,2} \qquad (1)$$

where m is the signal magnitude, given by

$$m = \frac{q_i - q_{min}}{q_{max} - q_{min}} \qquad (2)$$

and the first derivative of the instantaneous heat flux is found by the central-difference equation

$$q_i' = \frac{q_{i+1} - q_{i-1}}{2h} \qquad (3)$$

where h is the sampling period. This detector function is unique in that it incorporates the magnitude of fluctuations as well as the first derivative. The third trace is the criterion function. It is an exponentially-weighted centered moving average of the detector function, which is represented by

$$C_i = \frac{h^2}{1 + (\tau_s/h)} \sum_{j=i-(\tau_s/2h)}^{j=i+(\tau_s/2h)} w_j D_j \qquad (4)$$

where w_j is the weighting factor, defined by

$$w_j = e^{-[12.5\ |j-i|\ (\tau_s/h)]} \qquad (5)$$

and τ_s is the smoothing period. The smoothing period was in this case chosen to to be 10μs. This value corresponds to the upper limit of the heat-transfer-analog bandwidth (100kHz), and thus ensures that the smallest detectable turbulent spots are included in the analysis. The bottom trace in the figure is the intermittency signal, which is obtained by setting an appropriate threshold for the criterion function. In practice, the threshold is chosen by trial and error such that the resulting intermittency signal is a good representation of the original signal.

As stated previously, it is possible to obtain much important turbulent-spot information from the above procedure. First, the variation of intermittency through the transition zone can be determined. Second, it is possible to estimate turbulent-spot generation rates simply by counting the number of spots detected by the process. Finally, it is possible to determine spot leading- and trailing-edge convection velocities. This is because the intermittency signal (bottom trace in Figure 1) can be separated into two distinct signals. The first consists of the locations in time of turbulent-spot-leading-edge passage over the gauge, while the second is made up of the same for the trailing edges. These signals can then be crosscorrelated with the corresponding traces from gauges further down the plate. In this manner, it is possible to determine the trajectories of the turbulent-spot leading and trailing edges along the model surface.

Because a thin-film gauge integrates the heat-transfer distribution along its length, it is possible to make estimates of turbulent-spot lateral growth from the rate of change of thin-film gauge coverage with distance along the model surface. Figure 2 is an illustration of this process. It can be seen that the turbulent spot labelled A brings the instantaneous heat flux to a value somewhere between the laminar and

fully turbulent levels on the upper trace of Figure 2. This is because only a fraction of the total gauge length is covered by the spot. However, as the spot travels downstream, it is continually spreading in the cross-stream direction. As a result, the spot covers a greater percentage of the gauge whose trace is plotted in the bottom half of the figure. Knowing the gauge dispositions on the plate, it is possible to determine the location of the lateral edge of the turbulent spot over each gauge. Then, from simple geometry, the half-angle of spreading can be estimated.

Experimental Results

Figure 3 is a plot of the turbulent-spot trajectories resulting from the procedure described in the preceding section. The conditions of the run are zero pressure gradient, no grid, a gas-to-wall temperature ratio of 1.4, and a freestream Mach number of 0.55. Three trajectories are shown, and values of the percentages of the freestream velocity associated with each line are indicated. The 'mean' trajectory was calculated by the procedure outlined in Ref. 1. Figure 4 is a plot of spot trajectories for the same conditions as those above except that the freestream Mach number is 1.86. There is excellent agreement between the results of the two cases. Also, the results agree very well with those of Schubauer and Klebanoff (Ref. 3) for turbulent-spot leading- and trailing-edge convection velocities. It should be noted that this marks the first time that these parameters have been determined in natural transition at any conditions, let alone compressible Mach numbers.

There are some differences between the spot trajectories measured in zero and non-zero pressure gradients. Figure 5 is a plot of the pressure gradients for which data has been collected in this program, while Figure 6 is a set of turbulent-spot trajectories for the mild favorable pressure gradient case. Figure 7 is a plot of the variation of leading-edge, trailing-edge, and 'mean' convection velocities with distance along the model surface. For comparison, the variation of freestream velocity with

distance is also illustrated. It is evident that the leading-edge velocity is a roughly constant fraction of the freestream velocity, while the trailing-edge and 'mean' convection rates are not. Wygnanski (Ref. 4) found that neither the leading- nor the trailing-edge velocity scales directly with that of the freestream. In addition, he concluded that a turbulent spot which is formed in a zero pressure gradient has 'memory' of its conditions at formation and is unaffected by subsequent increases in freestream velocity. No evidence of that effect is manifest in the results of these experiments. This perhaps points to the dangers of relying on data gathered in artificially-generated spot experiments for gas-turbine applications.

Some preliminary estimates of the half-angle of turbulent-spot spreading at various conditions are presented in Table 1. It can be seen that the lateral growth of turbulent spots is greatly inhibited by a favorable pressure gradient and augmented by an adverse one. This is in general agreement with estimates of the effect of pressure gradient from artificial-spot studies, and it supports the conclusion of Gad-el-Hak, et al. (Ref. 5) that spots spread laterally by the local destabilization of the laminar boundary layer at their edges. Also, the value of 7.6° given for the half-angle at zero pressure gradient is for Mach 0.55. This value is lower than that generally accepted at incompressible Mach numbers (10-11°), and this supports the theoretical conclusion of Doorly and Smith (Ref. 6) that the spreading angle of a turbulent spot decreases monotonically as freestream Mach number increases.

Run Number	Pressure Gradient	Spot Half-Angle
4864	Zero	7.6°
4896	Mild Favorable	2.8°
4910	Strong Favorable	1.2°
4912	Mild Adverse	15.0°

Table 1 - Estimates of the half-angle of turbulent-spot spreading under various conditions.

Figure 8 is a plot of the variation of intermittency with distance along the flat-plate model surface for various pressure gradients. All three curves represent data gathered at an inlet unit Reynolds number of 6 million per meter and a gas-to-wall temperature ratio of 1.4. It can be seen that an adverse pressure gradient leads to a decrease in the length of the transition zone as compared to the zero pressure gradient case, while the opposite is true of a comparison between the favorable and zero pressure gradients. Indeed, in the case of the favorable pressure gradient, the intermittency changes only slightly over the measrurement interval represented in the figure. These results are also in general agreement with those presented in Table 1.

Conclusions

Naturally-occuring turbulent spots have been tracked in a boundary layer undergoing transition at gas-turbine representative conditions. Turbulent-spot generation rates, spreading angles, and leading- and trailing-edge convection velocities have been determined as a function of Mach number, pressure gradient, and freestream turbulence level. The results are potentially of great use to engine designers when coupled with a suitable modeling technique. A full exposition of the experimental results and modeling work will be presented in the dissertation of J.P. Clark, which will be submitted to the University in late 1992.

References

1- Clark, J.P., Jones, T.V., Ashworth, D.A., and LaGraff, J.E., 1991, 'Turbulent Spot Development in a Mach 0.55 Flow', *Proceedings of the Royal Aeronautical Society Boundary Layer Transition and Control Conference*, Cambridge, U.K., Vol. 1, pp. 21.1-21.9.

2- Hedley, T.B. and Keffer, J.F., 1974, 'Turbulent/Non-Turbulent Decisions in an Intermittent Flow', *Journal of Fluid Mechanics*, Vol. 64, Part 4, pp. 645-678.

3- Schubauer, G.B and Klebanoff, P.S., 1955, 'Contributions on the Mechanics of Boundary Layer Transition', NACA TN-3489.

4- Wygnanski, I., 1981, 'The Effects of Reynolds Number and Pressure Gradients on the Transitional Spot in a Laminar Boundary Layer', *Lecture Notes in Physics*, Vol. 136, pp. 304-332.

5- Gad-el-Hak, M., Blackwelder, R.F.. and Riley, J.J., 1981, 'On the Growth of Turbulent Regions in Laminar Boundary Layers', *Journal of Fluid Mechanics*, Vol. 110, pp. 73-95.

6- Doorly, D.J. and Smith, F.T., 1992, 'Initial-Value Problems for Spot Disturbances in Incompressible or Compressible Boundary Layers', *Journal of Engineering Mathematics*, Vol. 26.

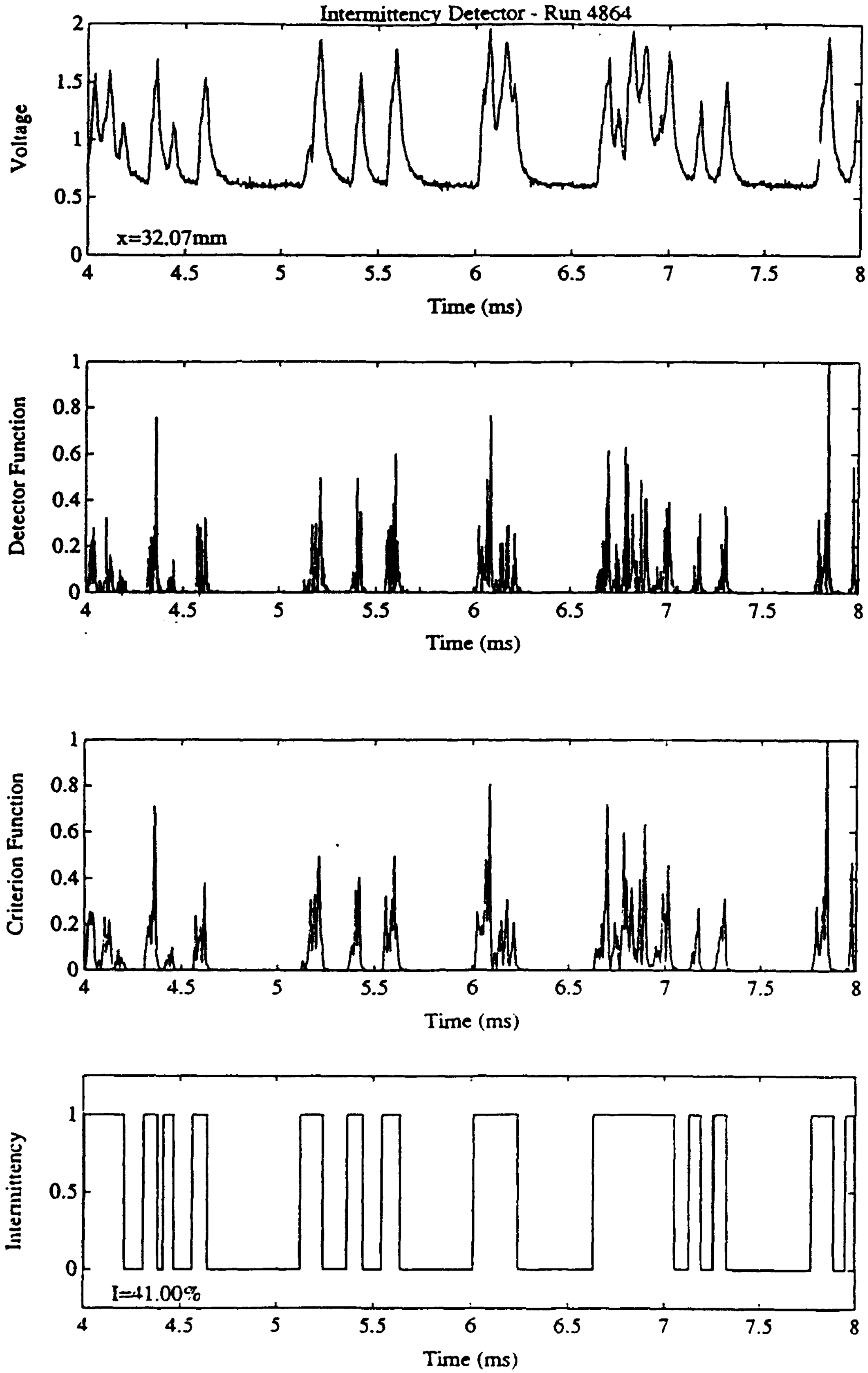

Figure 1 - Illustration of the intermittency detection procedure.

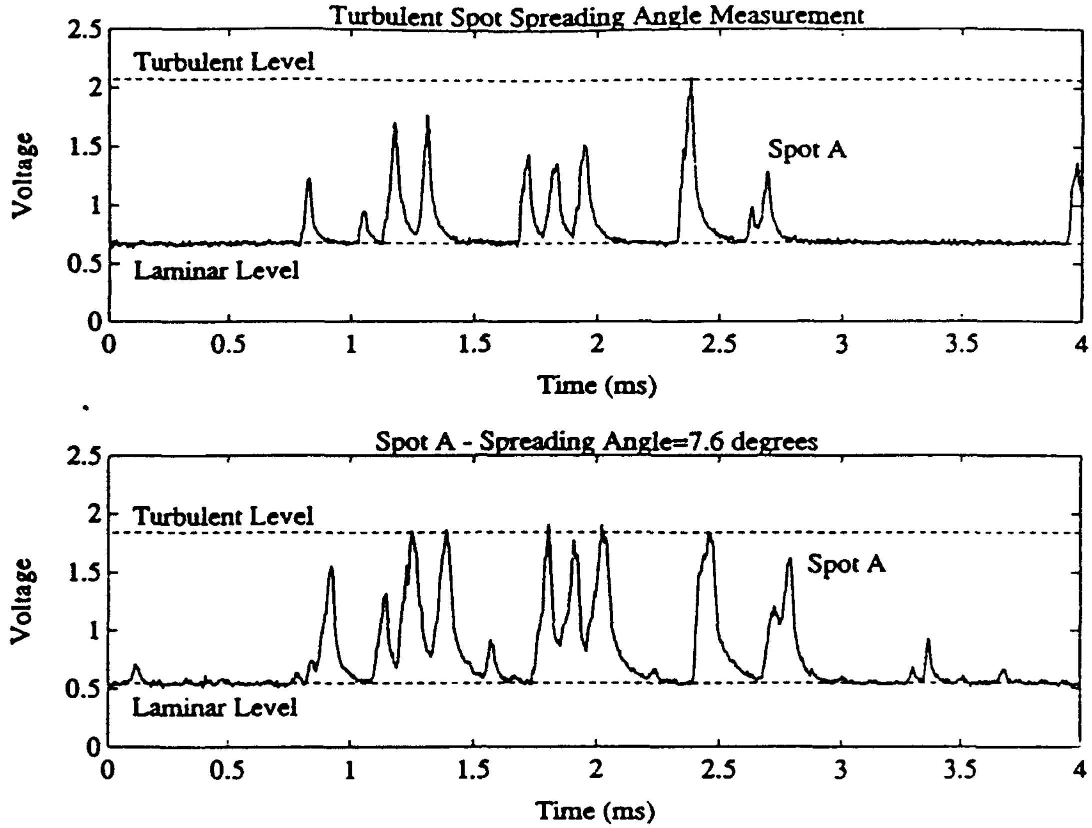

Figure 2 - Illustration of the procedure used to estimate the lateral growth rates of turbulent spots. The top trace is data from the thin-film gauge located at x=24.11mm, while the bottom one is from the gauge at x=36.06mm.

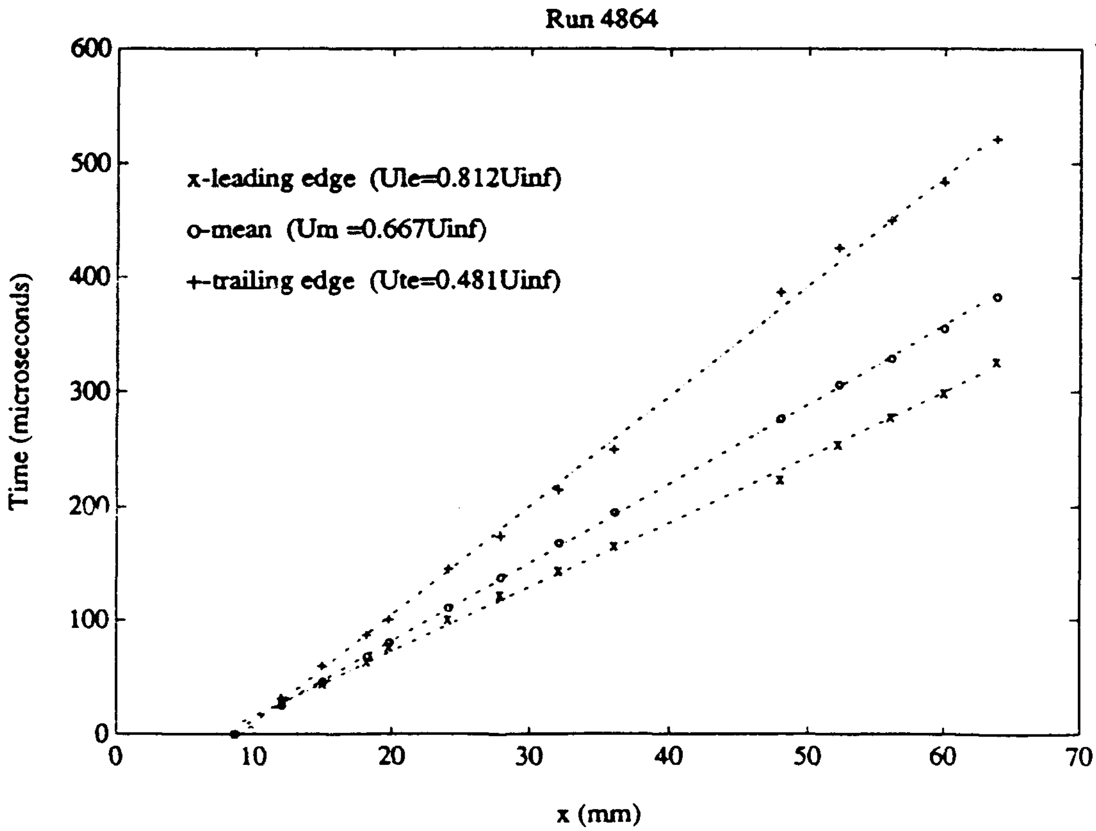

Figure 3 - Turbulent spot trajectories for Mach 0.55, zero pressure gradient flow with no grid and a gas-to-wall temperature ratio of 1.4.

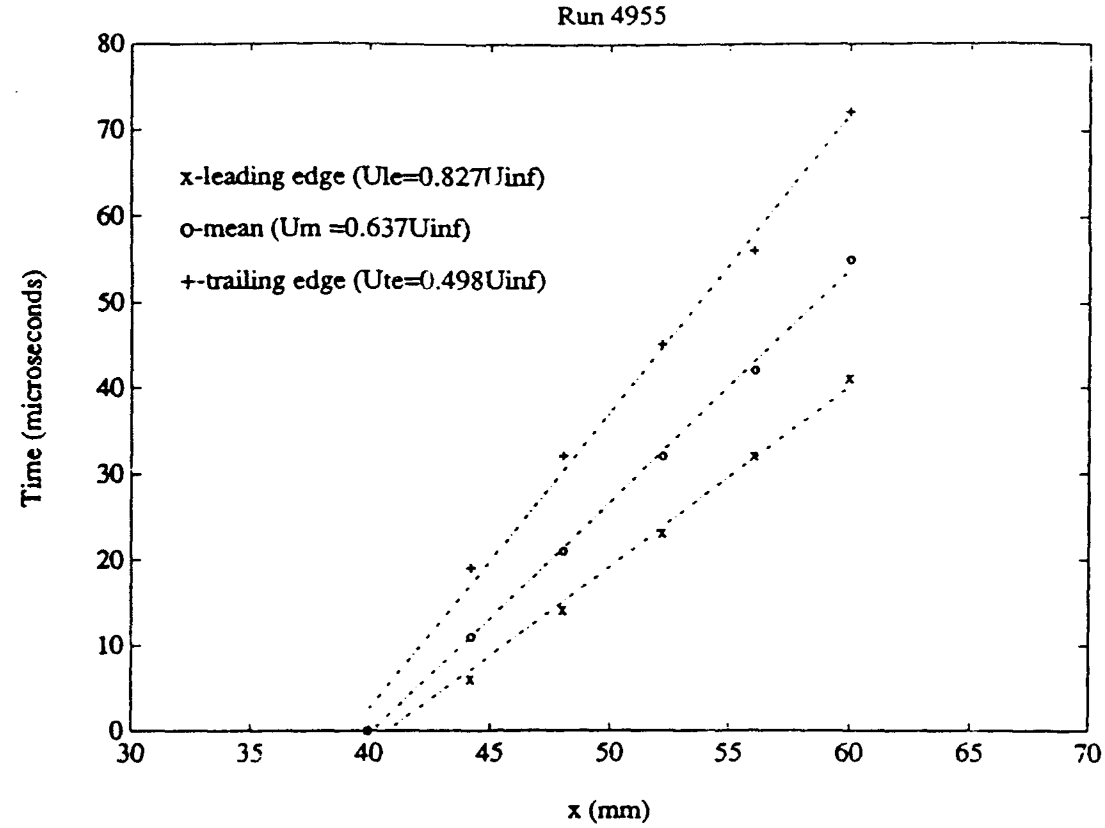

Figure 4 - Turbulent spot trajectories for Mach 1.86, zero pressure gradient flow with no grid and a gas-to-wall temperature ratio of 1.4.

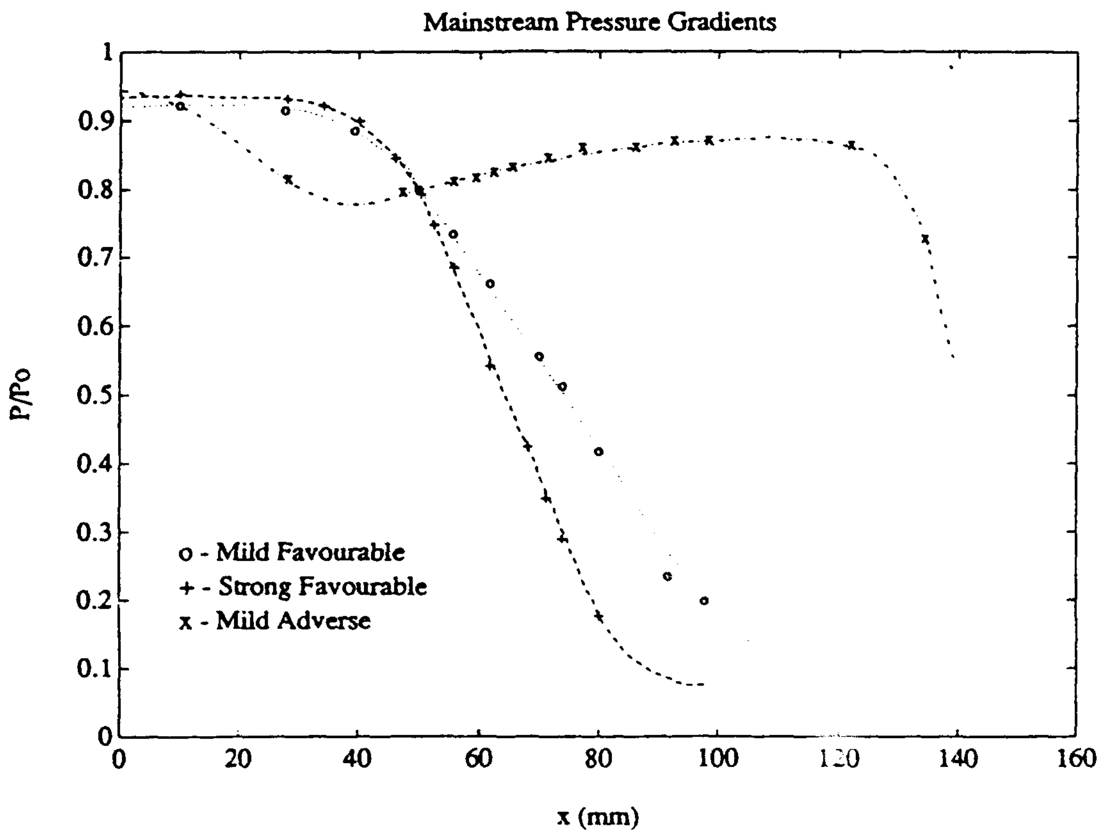

Figure 5 - Mainstream pressure gradients for which transition data has been collected.

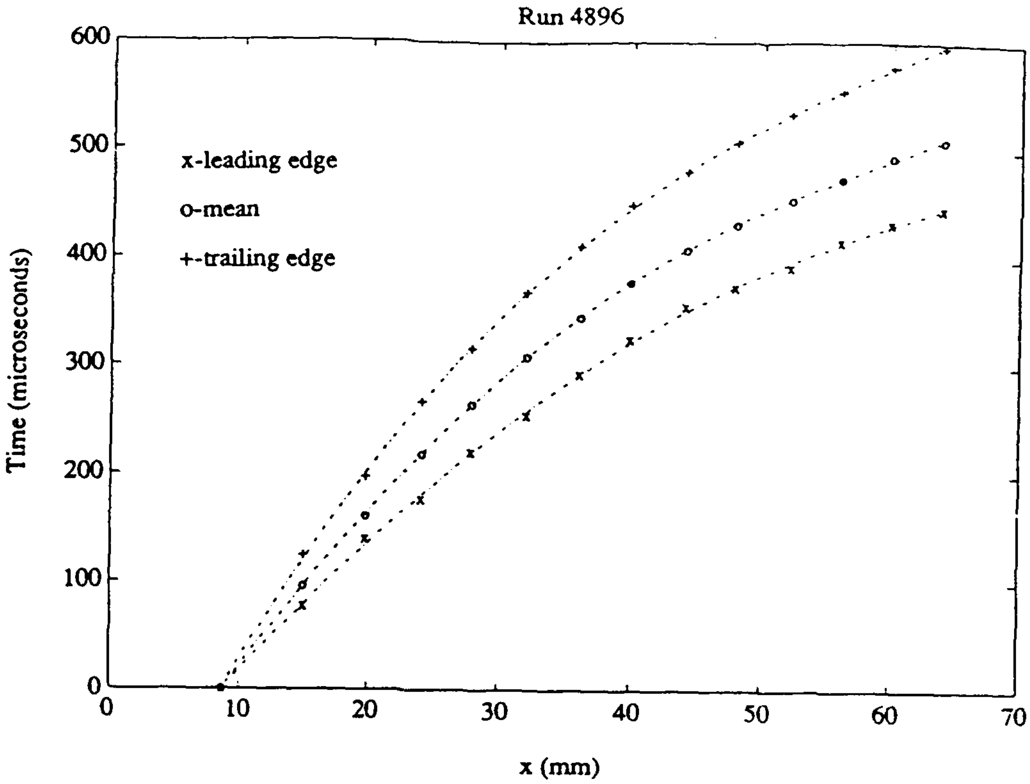

Figure 6 - Turbulent spot trajectories obtained during a run with the mild favorable pressure gradient liner (no grid, gas-to-wall temperature ratio of 1.4).

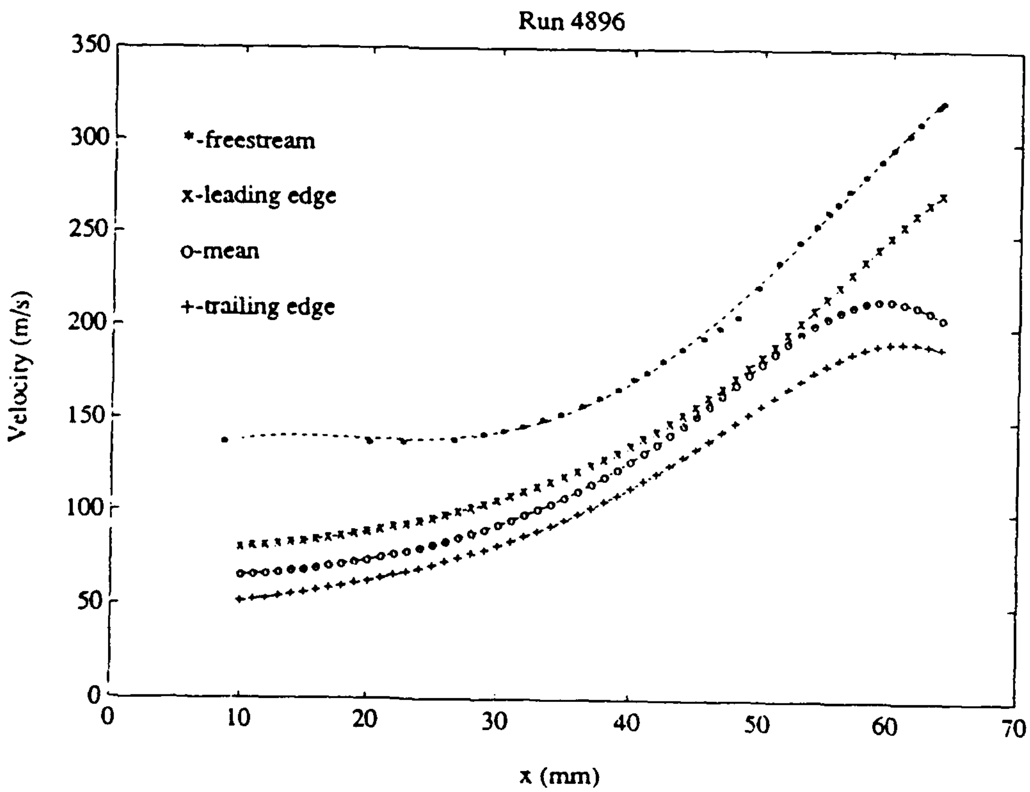

Figure 7 - The variation of turbulent spot convection rates with distance from the leading edge for the mild favorable pressure gradient case.

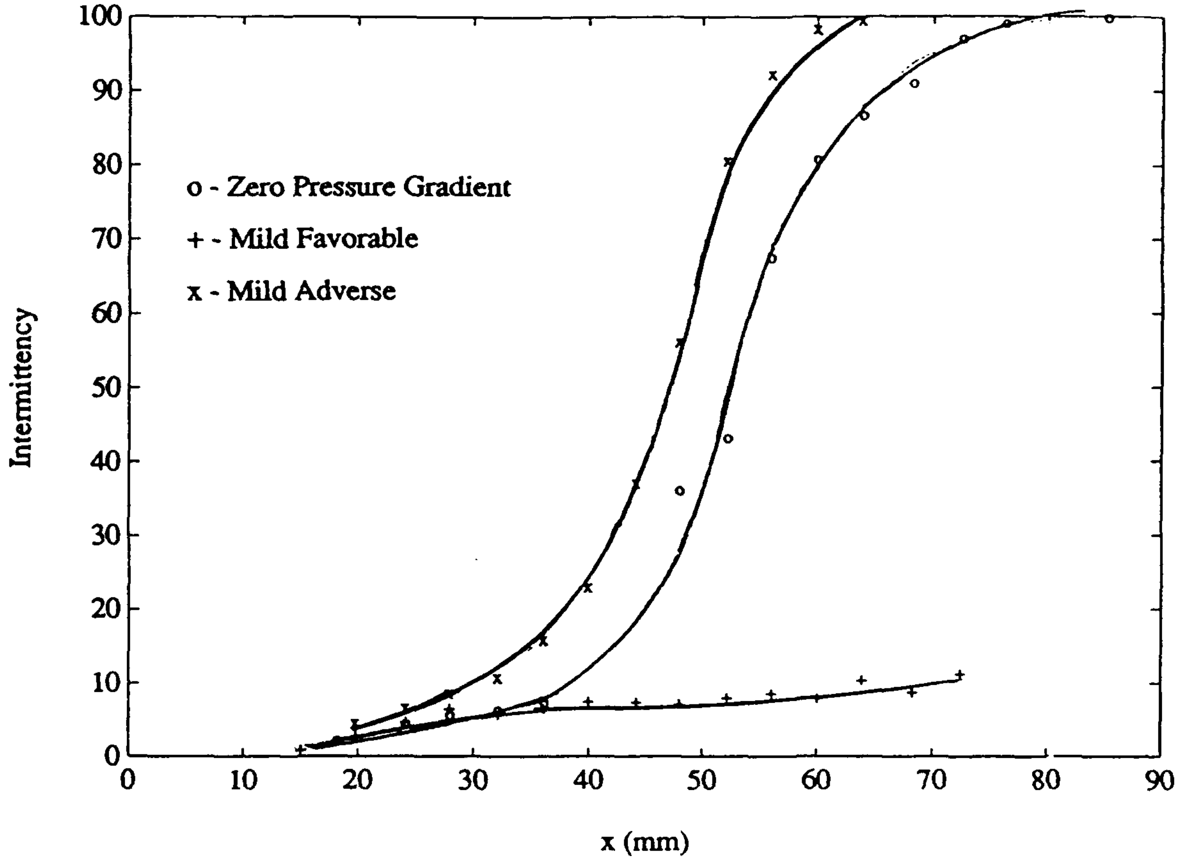

Figure 8 - The variation of intermittency with distance downstream from the leading edge at various pressure gradients. In all cases, Re_u=6.0E+06/m, T_g/T_w=1.4, and no turbulence grid is present upstream of the plate.

TURBULENT SPOT DEVELOPMENT IN A MACH 0.55 FLOW

J.P. Clark and T.V. Jones, Oxford University, Oxford, U.K.
D.A. Ashworth, Rolls-Royce, Bristol, U.K.
J.E. LaGraff, Syracuse University, Syracuse, NY, U.S.A

Abstract

An experimental investigation of the end stage of the boundary layer transition process has been conducted. The convection rates of naturally occuring turbulent spots were determined in a transient aerodynamic facility using simultaneous, multichannel, wide bandwidth (100kHz) surface heat transfer rate instrumentation. The experimental conditions are able to simulate many of the important parameters associated with modern gas turbine blades, viz., transonic Mach number, high unit Reynolds number, high gas to wall temperature ratio, various pressure gradients, and varying freestream turbulence intensities. Initial results of tests at a freestream Mach number of 0.55 under conditions of zero pressure gradient, gas to wall temperature ratio of 1.4, and two freestream turbulence intensities are presented here.

The data was collected on a flat plate model with surface thin film heat transfer gauges placed at various locations. Turbulent spots have been tracked with this model in place, and the results are presented here. In addition, time mean data has been recorded on the model and compared with standard flat plate correlations for heat transfer with good results.

The passage of turbulent spots over thin film gauges was used to characterise naturally occuring turbulent spots. Firstly, the simultaneous measurement of surface heat flux at sixteen locations permitted the tracking of individual turbulent spots through the transition zone. Secondly, cross-correlation analysis between channels lead to estimates of mean spot convection rates along the model surface which were at levels comparable with low speed measurements. Finally, intermittency distributions were calculated from the instantaneous heat transfer signals through the transition zone. The results presented in this paper represent the first phase of an experimental programme which will enable the above parameters to be determined for realistic aerodynamic environments.

Nomenclature

CCF	crosscorrelation coefficient
f_{max}	analogue upper frequency limit
k	thermal conductivity
l_{min}	minimum detectable spot length
M_∞	freestream Mach number
Nu_x	Nusselt number
Pr	Prandtl number
q	heat flux
q_m	mean heat flux
Re_u	unit Reynolds number $(\rho_\infty U_\infty)/\mu_\infty$
Re_x	Reynolds number $(\rho_\infty U_\infty x)/\mu_\infty$
T_o	freestream total temperature
T_w	wall temperature
T_m	mean thin film temperature
t	time
U_{spot}	turbulent spot convection rate
U_∞	freestream velocity
x	distance from flat plate leading edge
z	distance of thin film gauge center from the flat plate centerline
α	spot spreading angle
γ	intermittency
δ	boundary layer thickness
μ_∞	freestream dynamic viscosity
ρ_∞	freestream density

Introduction

Ever since Emmons first advanced the theory of transition by turbulent spots in 1950 (Ref. 1), an ever increasing amount of research has been devoted to the study of turbulent spot characteristics. Schubauer and Klebanoff (Ref. 2), who first confirmed Emmons' theory of transition by turbulent spots, provided the first detailed measurements of turbulent spot convection rates and spreading angles. The principal results of their work are shown in Figure 1. Their experiments, as well as those of many other researchers since then (Ref. 3-7), have centered on the study of artificially generated turbulent spots in an otherwise laminar boundary layer at very low freestream velocities. The goal of the present study is to provide much of the same information concerning naturally occuring turbulent spots at conditions representative of the gas turbine environment.

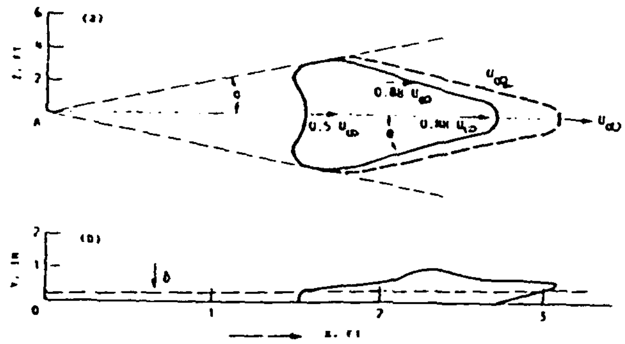

Figure 1 - Turbulent spot as measured by Schubauer and Klebanoff (Ref 2).

Much of the boundary layer on the suction surface of a gas turbine blade can be transitional. Consequently, a knowledge of the location and extent of the transition zone is necessary for the proper design of gas turbine blades. Without such information, gross errors can be made in regard to the total heating load on the blades. This is because of the tremendous difference between the heat transfer characteristics of laminar and turbulent boundary layer flows. This difference not only affects heat transfer estimates, but can also serve to distinguish between the two types of flow in an experiment involving surface thin film heat transfer gauges.

The use of thin film gauges for the determination of heat transfer rates in turbine representative flows is well established. A unified theory for the operation of thick and thin film gauges can be found in Schultz and Jones (Ref. 8), while a review of the aerodynamic interpretation of signals from thin films is presented in Oldfield and Ainsworth (Ref. 9). The use of thin films to detect boundary layer transition is also not new, and this technique has been used in the past at Oxford, most notably by Owen (Ref. 10), Doorly (Ref. 11), LaGraff, et al. (Ref. 12), and Ashworth, et al. (Ref. 13,14). Ashworth et al. (Ref. 13,14) performed transition experiments on the suction surface of a gas turbine rotor in a two-dimensional cascade under the influence of freestream turbulence and simulated nozzle guide vane wakes and shocks. A typical result of their work is seen in Figure 2.

It is clear from Figure 2 that much information can be obtained from the simultaneous measurement of instantaneous surface heat flux at a number of positions along a model surface. First, the increase in heat transfer rate above the laminar level with turbulent spot passage is readily apparent. Second, the tracking of individual turbulent spots along the surface is plainly visible. Also, it is evident how intermittency can be calculated simply by setting a threshold for an individual signal slightly above the laminar level and determining the fraction of the total measurment interval that the heat transfer coefficent is above that threshold.

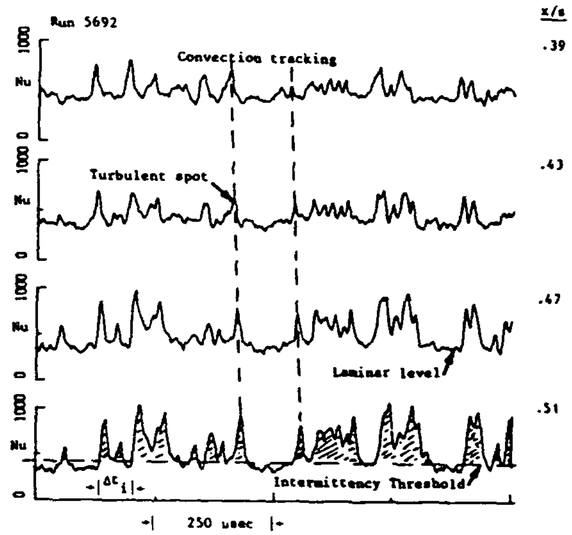

Figure 2 - Typical transition results from Ashworth et al. (Ref. 14).

The transition process in gas turbines is influenced by a variety of different mechanisms. Most notably, these are freestream turbulence intensity, surface roughness, heat transfer, compressibility, pressure gradient, and surface curvature. The aim of this work is to determine the influence of some of these characteristics on the formation and growth of turbulent spots in a naturally transitioning boundary layer at engine representative conditions. Effects of freestream turbulence intensity, pressure gradient, and compressibility will all be determined separately at turbine representative Reynolds numbers and gas to wall temperature ratios. This paper presents, as initial results of the experimental program, a demonstration of the capability of the method to gather detailed transition data as well as evidence of the influence of freestream turbulence intensity on the formation and growth of turbulent spots.

Experimental Approach

The tests were conducted in the Oxford University 6 inch Isentropic Light Piston Tunnel (ILPT) as described by Jones, et al.

(Ref. 15). The ILPT is a transient facility which is capable of producing a flow with a range of Reynolds numbers, Mach numbers, and gas to wall temperature ratios in order to simulate conditions in modern gas turbine engines. Specifically, for the current tests, the Reynolds number of the flow was chosen to spread the transition zone over much of a flat plate model's length at $M_\infty=0.55$ and $T_0/T_W=1.4$.

A schematic of the 6 inch ILPT is seen in Figure 3(a). Its major components are the high pressure reservoir, pump tube with light piston, working section, and dump tank. During a tunnel run, air is suddenly injected into the pump tube from the high pressure reservoir through the ball valves indicated. This forces the piston down the pump tube, compressing the gas isentropically, and thus increasing its temperature. When the gas in the tube reaches the required pressure, the fast acting gate valve is opened and the air flows through the test section and into the dump tank in a total running time of roughly 300ms. If the volumetric rate of flow into the pump tube from the reservoir equals that flowing through the test section the total pressure and temperature during the run remain constant, and the run is said to be matched.

The freestream turbulence intensity in the ILPT was varied in this study by placing a parallel bar grid some 100mm upstream of the center of the working section. The grid was designed on the considerations of Roach (Ref. 16) and produced a measured freestream tubulence intensity of 0.5% at the center of the test section. Without the turbulence grid in place, the measured freestream turbulence intensity was 0.1%.

During this study, the working section of the ILPT was fitted with a flat plate model and boundary layer bleed apparatus (Figure 3(b)). To detect the presence of turbulent spots in the boundary layer, this model was instrumented with 39 platinum thin film heat transfer gauges. The locations of the gauges are given in Table 1, while a photograph of the flat plate itself is shown in Figure 4. The data presented here was collected with most of the 25 thin films located roughly on the model centerline. The remaining gauges are offset from the centerline and will be used later in the experimental program to determine the spreading angles of turbulent spots under various conditions.

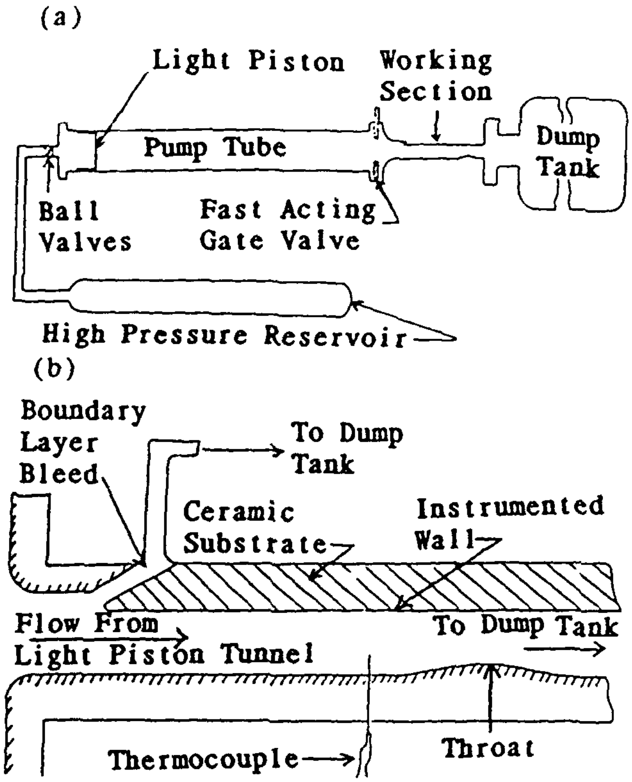

Figure 3 - Schematic of 6 inch ILPT.
(a) tunnel itself
(b) working section

Table 1 - Thin Film Gauge Locations. Gauges with $0.0 \le z \le 1.1$ are considered "centerline" gauges.

TFG#	x (mm)	z (mm)	TFG#	x (mm)	z (mm)
1	1.73	0.105	21	49.96	-1.740
2	8.63	0.340	22	52.18	0.150
3	12.04	0.350	23	54.04	2.790
4	15.01	0.485	24	56.04	0.480
5	18.19	1.075	25	58.00	-2.165
6	19.81	1.005	26	60.00	0.310
7	21.96	3.250	27	62.16	3.110
8	24.11	0.630	28	63.95	0.100
9	26.36	-2.295	29	66.34	-2.495
10	27.90	0.470	30	68.25	0.200
11	30.02	3.315	31	70.00	2.975
12	32.07	0.535	32	72.46	0.020
13	34.02	-2.400	33	74.37	-2.540
14	36.06	0.340	34	76.28	0.520
15	38.02	2.485	35	79.84	0.350
16	39.93	0.475	36	85.17	0.290
17	42.34	-2.640	37	90.17	0.290
18	44.18	0.190	38	95.15	0.130
19	46.15	1.730	39	100.00	0.020
20	48.00	0.845			

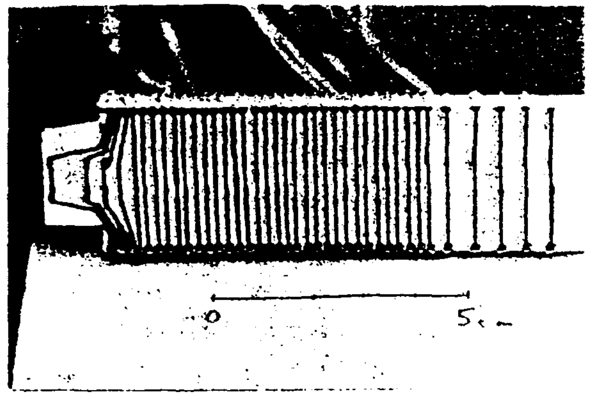

Figure 4 - Flat plate model instrumented with platinum thin film gauges. Leading edge is at left.

The use of thin film gauges for the measurement of steady and unsteady heat transfer rates is described in Ref. 8. The thin films used in this study were operated at a constant current and the signals from the gauges were processed through electrical analogues of the 1-d unsteady conduction equation. The analogues used are based on the design of Oldfield, et al. (Ref. 17) and have a nominal bandwidth of 0.1-100kHz.

Since the working range of the analogues has an upper frequency limit, the size of detectable turbulent spots must have a lower limit. The minimum detectable turbulent spot length is given by the equation

$$(1) \qquad l_{min} = U_{spot}/f_{max}$$

where Uspot and fmax are the spot convection rate and upper analogue frequency limit (100kHz), respectively. At a gas to wall temperature ratio of 1.4 with a freestream Mach number of 0.55 the minimum detectable spot length is 1.5mm, assuming that the mean convection rate of the spot is $0.69U_{\infty}$.

During any tunnel run, both fluctuating and time mean heat flux measurements were made as well as time mean pressure and temperature measurements. Fluctuating heat transfer rates were recorded simultaneously on 16 channels of A/D converters with 12 bit resolution, a maximum sampling rate of 1MHz, and a storage capacity of 64K per channel. In addition, time mean heat transfer rates were determined from data recorded on 32 channels of A/D converters with a maximum sampling rate of 15kHz. Mean heat transfer coefficients are presented as Nusselt number, defined as

$$(2) \qquad Nu_x = \frac{q_m}{T_o - T_m}\frac{x}{k}$$

where the gas conductivity, k, is described by the equation $k=0.0047+7.0E\text{-}5T_o$ in W/mK.

Results

The mean heat transfer results for the flat plate surface are shown in Figure 5 for the no grid and 0.5% turbulence grid cases as a plot of Nu_x vs. Re_x. The earlier transition brought about by the presence of freestream turbulence from the grid can be clearly seen. For comparison, standard correlations of the distribution of Nu_x with Re_x along a flat plate with an initially isothermal wall and constant freestream velocity taken from Kays and Crawford (Ref. 18) have been drawn on the plot. There is indeed good agreement between the theoretical and experimental results.

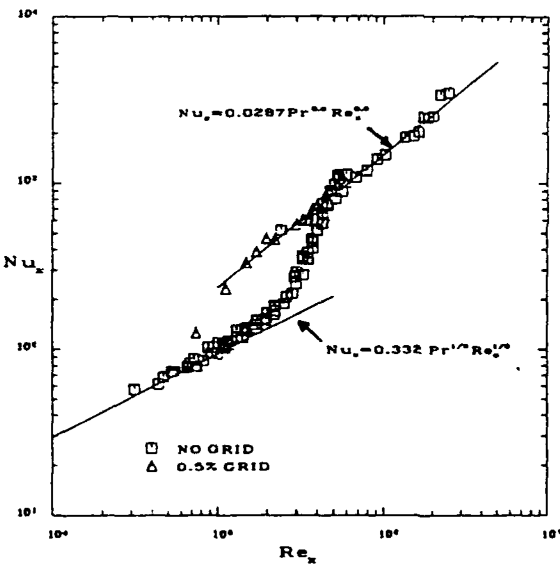

Figure 5 - Mean heat transfer results for no grid and 0.5% turbulence grid cases.

The effect of freestream turbulence on the transition zone is also evident from a comparison of Figures 6 and 7. Figure 6 is a set of 16 simultaneously measured heat flux traces from gauges located at various streamwise distances along the flat plate for the no grid case, while Figure 7 shows traces from the same gauges measured with the grid in place. For both runs, the freestream unit Reynolds number, Re_u, was 6E+06/m and $T_o/T_w=1.4$. It is readily apparent from the character of the traces that the transition process was accelerated by the

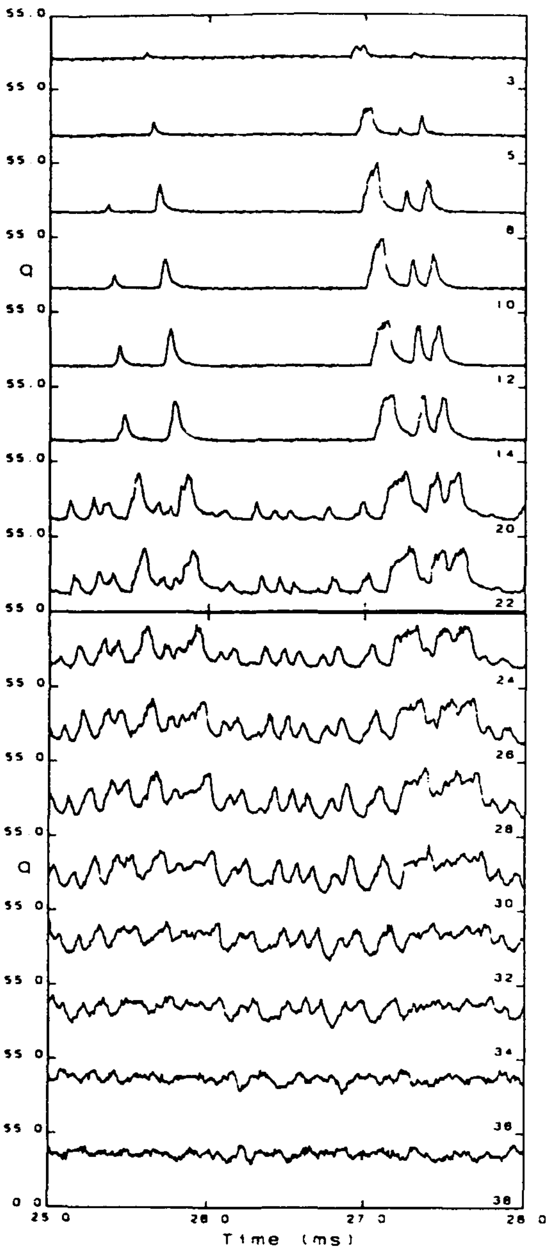

Figure 6 - Instantaneous heat transfer traces (q in kW/m²). Re_u=6E6/m, T_O/T_W=1.4, No Grid. (Thin film gauge number is in lower right hand corner of each trace. See Table 1)

presence of turbulence from the grid. In fact, the very first measuring station shown (gauge #3) is deep in the transition zone in Figure 7, while it is almost completely laminar in the no grid case. Furthermore, the heat flux traces for the no grid case do not appear to have a fully turbulent character until gauge #34, while the flow is clearly fully turbulent by gauge #5 with the grid in place.

Several features of the heat flux traces presented in Figures 6 and 7 are dramatically illustrated in Figure 8, which is an expanded scale version of two of the heat flux traces seen in Figure 6. First, the apparent time shift of the trace from gauge 10 to gauge 14 associated with the convection of the turbulent events can be clearly seen. Second, the data from gauge 14 is compared with theoretical values of the laminar and turbulent heat fluxes at the given measuring station

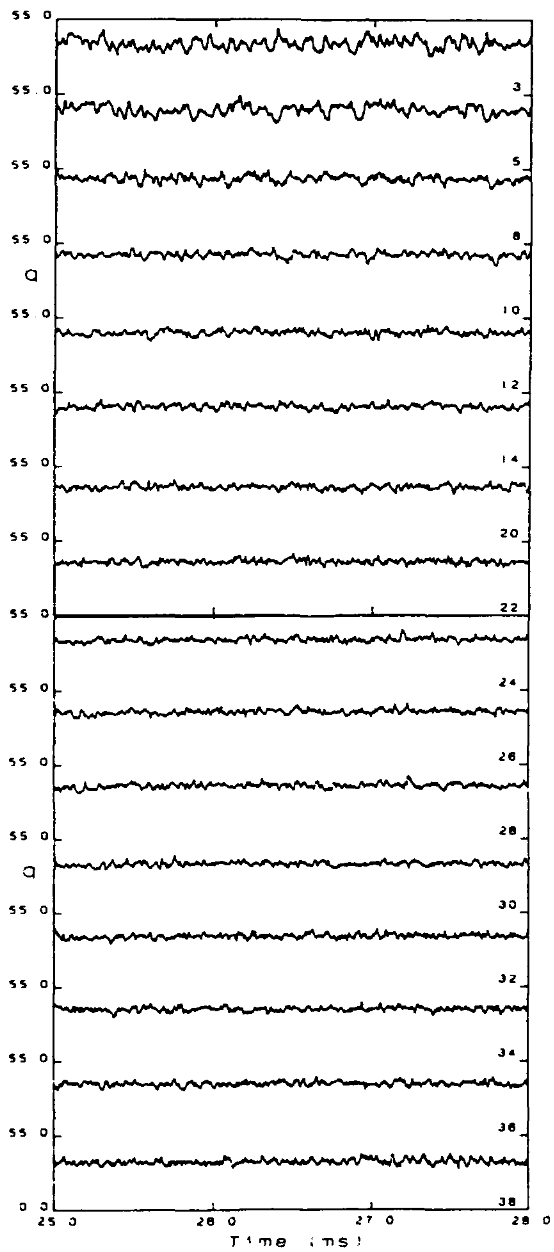

Figure 7 - Instantaneous heat transfer traces, (q in kW/m²). Re_u=6E6/m, T_O/T_W=1.4, 0.5% Grid.

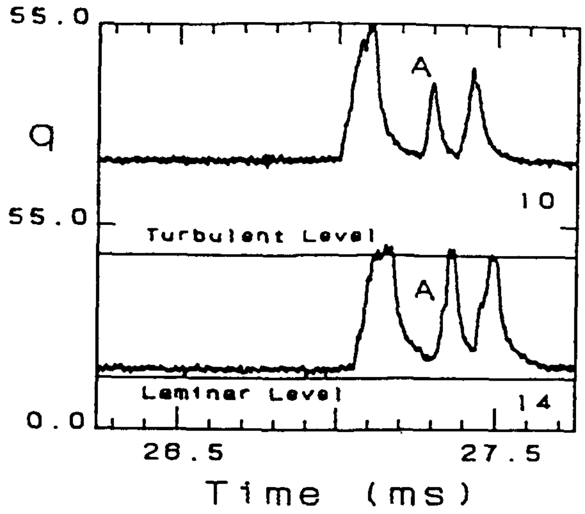

Figure 8 -Expanded scale heat transfer traces, (q in kW/m²). Re_u=6E6/m, T_O/T_W=1.4, No Grid.

(again from Ref. 18) with good results. The theoretical value of the turbulent heat flux was calculated assuming that the origin of the turbulent boundary layer was coincident with the origin of the first detectable turbulent spots, as suggested by Narasimha (Ref. 19). For this run, turbulent spots were first detected on gauge 3, giving a turbulent boundary layer origin at x≈12.0mm. In addition, the characteristic sharp rise in heat flux with the passage of the spot leading edge as compared to the slower relaxation to the laminar value with the passage of the spot trailing edge is clearly evident. This feature of turbulent spot data, which is indicative of the higher transport efficiency of turbulence, was first noticed in the hot wire traces of Schubauer and Klebanoff (Ref. 2). Finally, the effect of turbulent spot growth on the heat flux traces can be seen in the figure. In the trace from gauge 10, the spot labeled A in the figure does not cause the heat flux level to reach the fully turbulent value. This is because the thin film, which effectively integrates the heat flux distribution over its length, is only partially covered by the turbulent spot. However, by the time the spot has reached gauge 14, it has grown laterally to such an extent that it completely covers the gauge, and thus brings the heat transfer level to the full turbulent value.

The effect of freestream turbulence intensity on transition is further illustrated in Figure 9, which is a plot of intermittency, γ, through the transition zone versus Re_x for both the no grid case and the 0.5% grid case. The intermittencies plotted in the figure were obtained from the method illustrated in Figure 2 and described in the Introduction of this report.

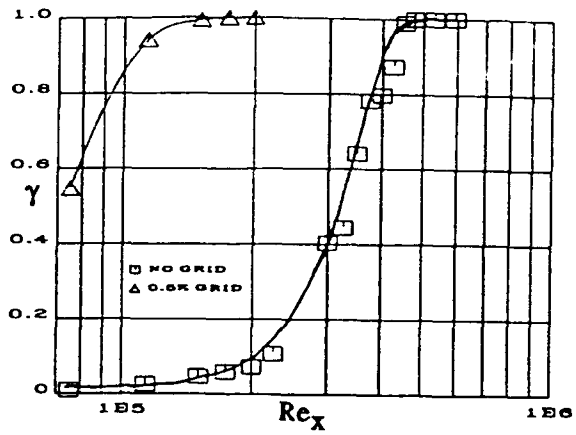

Figure 9 - Intermittency distribution through the transition zone for both the No Grid and 0.5% Grid cases.

Mean turbulent spot convection rates through the transition zone were determined via the method depicted in Figure 10. Two simultaneously recorded heat flux traces from the no grid run of Figure 6 are shown in part (a) of the figure, while part (b) shows the results of a crosscorrelation analysis performed on the two signals. The maximum crosscorrelation coefficient is roughly 0.95, and this occurs at a time lag of 32µs. From the known distance between the gauges, it was determined that the mean convection rate of turbulent spots from gauges 28-30 was $0.65U_\infty$. This same analysis was applied from gauge to gauge along the plate from the origin of the first detectable turbulent spots to the end of the transition zone. The results of these calculations are plotted in Figure 11 for the no grid case as turbulent spot trajectories. A least squares line fit was applied to the experimental points and the results of this also indicated that the mean turbulent spot convection rate was $0.65U_\infty$. For comparison, the spot leading and trailing edge velocities determined by Schubauer and Klebanoff (Ref. 2) are also plotted on the figure. Although at present no attempt has been made to determine spot leading and trailing edge celerities, the mean convection rate is near the average of commonly accepted values from low speed measurements and in good agreement with the results of Ashworth, et al. (Ref. 14).

(a)

(b)

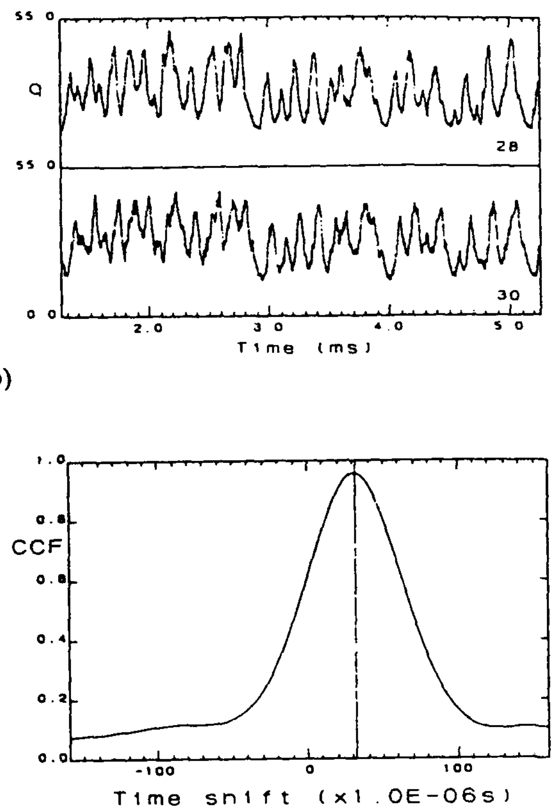

Figure 10-Example of crosscorrelation analysis of adjacent heat transfer traces used in spot convection rate calculations. Peak CCF of 0.95 at 32μs time lag.

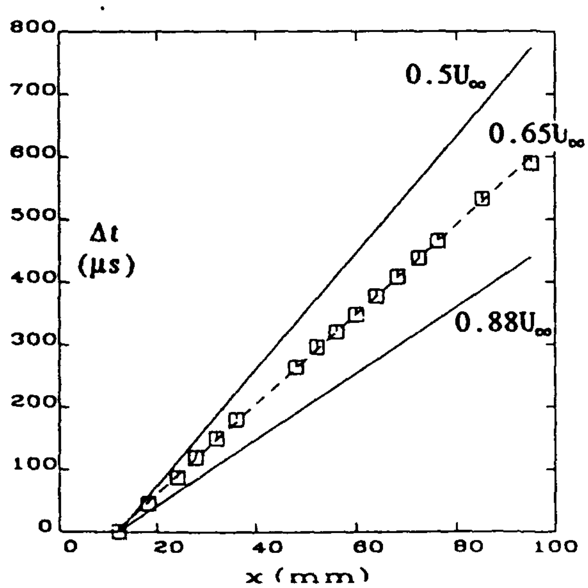

Figure 11 - Turbulent spot trajectory for the No Grid case (Re_u=6E6/m, T_O/T_W=1.4).

Since the boundary layer was almost fully turbulent from the leading edge of the plate at Re_u=6E+06/m with the turbulence grid in place, another set of data was taken at Re_u=5E+06/m. The mean heat transfer results of this run are also plotted in Figure 5, and account for the points early in the transition zone. Instantaneous heat flux traces are shown in Figure 12, where the boundary layer is seen to undergo a nearly complete transition to turbulence over the distance represented in the figure. The traces appear to have much the same character as those of the no grid case, and crosscorrelation analysis of the data in Figure 12 resulted in the spot trajectory plot of Figure 13. The mean convection rate in this case was found to be $0.64U_\infty$, which is in good agreement with the no grid results.

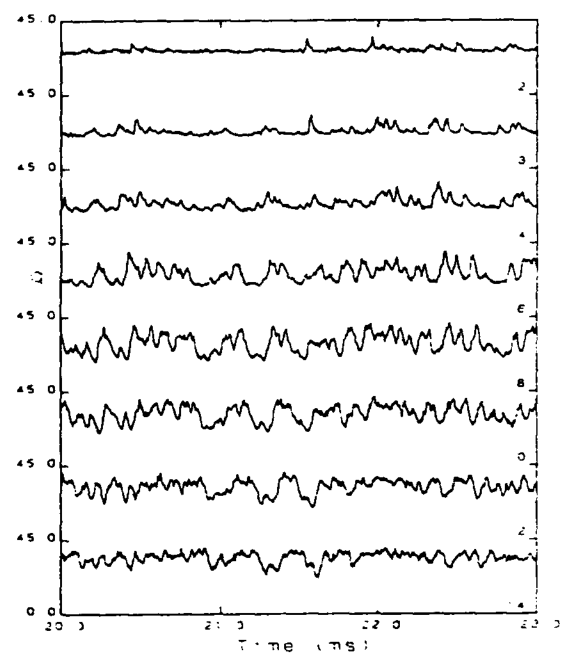

Figure 12 -Instantaneous heat transfer traces, (q in kW/m²). Re_u=5E6/m, T_O/T_W=1.4, 0.5% Grid.

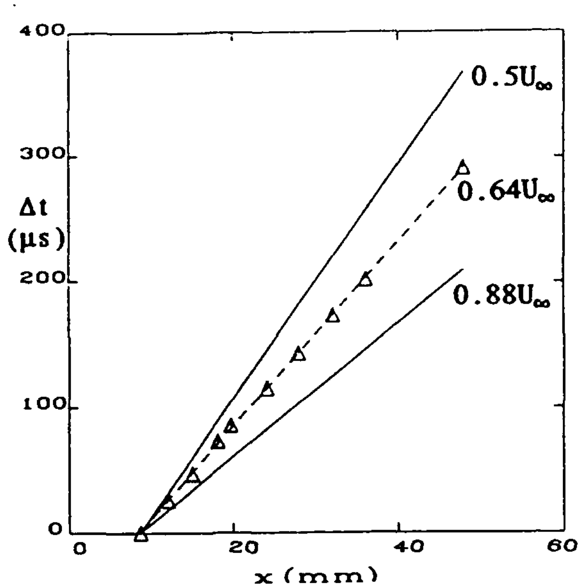

Figure 13 - Turbulent spot trajectory for the 0.5% Grid case (Re_u=5E6/m, T_0/T_w=1.4).

Conclusions

Turbulent spots have been tracked in a flat plate boundary layer using an Isentropic Light Piston Tunnel, wide bandwidth heat transfer instrumentation, and A/D converters operating with a sampling rate of 1MHz. From instantaneous heat flux measurements made simultaneously through much of the transition zone, it was possible to determine the intermittency of the boundary layer at each measuring station. Also, crosscorrelation analysis of signals from adjacent thin films resulted in very high crosscorrelation coefficients and mean turbulent spot convection rates in natural transition at engine representative conditions which were in close agreement with data from other studies. Increasing the level of freestream turbulence caused the boundary layer to undergo transition at a lower Reynolds number, but seemed to have little effect on mean spot convection rates. In addition, mean heat transfer rates were in good agreement with standard flat plate correlations.

Acknowledgements

This work was sponsored under Grant #89-0427 from the United States Air Force Office of Scientific Research. The program technical monitors were Capt. Hank Helin, Dr. James McMichael, and Major Dan Fant. Their support is kindly acknowledged. Special thanks is due to Mr. T. Godfrey, whose expert craftsmanship was employed in the construction of the flat plate model and test section walls. Special thanks is due also to S.R. Smelser for help in the production of some of the figures.

References

1- Emmons, H.W., "The Laminar-Turbulent Transition in a Boundary Layer - No. I," *Journal of Aeronautical Sciences*, Vol. 18, pp. 490-498, 1951.

2- Schubauer, G.B. and Klebanoff, P.S., "Contributions on the Mechanics of Boundray Layer Transition," *NACA TN-3489*, 1955.

3- Cantwell, B., Coles, D., and Dimotakis, P., "Structure and Entrainment in the Plane of Symmetry of a Turbulent Spot," *Journal of Fluid Mechanics*, Vol. 87, No. 4, pp. 641-672, 1978.

4- Elder, J.W., "An Experimental Investigation of Turbulent Spots and Breakdown to Turbulence," *Journal of Fluid Mechanics*, Vol. 9, pp. 235-246, 1962.

5- Gad-el-Hak, M., Blackwelder, R.F., and Riley, J.J., "On the Growth of Turbulent Regions in Laminar Boundary Layers," *Journal of Fluid Mechanics*, Vol. 110, pp. 73-95, 1981.

6- Wygnanski, I., Sokolov, M., and Friedman, D., "On a Turbulent 'Spot' in a Laminar Boundary Layer," *Journal of Fluid Mechanics*, Vol. 78, No. 4, pp. 785-819, 1976.

7- Katz, Y., Seifert, A., and Wygnanski, I., "On the Evolution of the Turbulent Spot in a Laminar Boundary Layer with a Favourable Pressure Gradient," *Journal of Fluid Mechanics*, Vol. 221, No. 12, pp. 1-22, 1990.

8- Schultz, D.L, and Jones, T.V., "Heat Transfer Measurements in Short Duration Hypersonic Facilities," NATO Advisory Group for Aeronautical Research and Development AGARDOGRAPH 165, 1973.

9- Oldfield, M.L.G., and Ainsworth, R.W., "The Use of Wide Bandwidth Heat Transfer Gauges to Diagnose Unsteady Turbomachinery Flows," *Proceedings of the Symposium on*

Measuring Techniques in Transonic ana Supersonic Cascade Flow, C.E.R.L., 1988.

10- Owen, F.K., "Transient Experiments on a Flat Plate at Subsonic and Supersonic Speeds," *AIAA Journal*, Vol. 8, No. 3, pp. 518-523, 1970.

11- Doorly, D.J., "A Study of the Effects of Wake Passing on Turbine Blades," D.Phil Thesis, Oxford University, 1983.

12- LaGraff, J.E., Ashworth, D.A., Schultz, D.L., "Measurement and Modelling of the Gas Turbine Blade Transition Process as Disturbed by Wakes," *ASME Journal of Turbomachinery*, Vol. 111, No. 7, pp. 315-322, 1989.

13- Ashworth, D.A., LaGraff, J.E., and Schultz, D.L., "Unsteady Interaction Effects on a Transitional Turbine Blade Boundary Layer," *ASME Journal of Turbomachinery*, Vol. 111, April, pp. 162-168, 1989.

14- Ashworth, D.A. and LaGraff, J.E., "Measurement and Modelling of Turbulent Spot Growth on a Gas Turbine Blade," *AIAA 89-0328*, 1989.

15- Jones, T.V., Schultz, D.L., and Hendley, A.D., "On the Flow in an Isentropic Light Piston Tunnel," ARC 34217, 1973.

16- Roach, P.E., "The Generation of Nearly Isotropic Turbulence by Means of Grids," *International Journal of Heat and Fluid Flow*, Vol. 8, No. 2, 1983.

17- Oldfield, M.L.G., Burd, H.J., and Doe, N.G., "Design of Wide-Bandwidth Analogue Circuits for Heat Transfer Instrumentation in Transient Tunnels," *16th Symposium of ICHMT*, Bubrovnik, Hemisphere Publications, 1982.

18- Kays, W.M. and Crawford, M.E., *Convective Heat and Mass Transfer*, McGraw-Hill, New York, NY, 1980.

19- Narasimha, R., "The Laminar-Turbulent Transition Zone in the Boundary Layer," *Progress in Aerospace Sciences*, Vol. 22, pp. 29-80, 1985.

Appendix II

AGARD Meeting on Heat Transfer and Cooling in Gas Turbines

Measurement of Turbulent Spots and Intermittency Modelling at Gas Turbine Conditions

Clark, J.P., Oxford University, Oxford, U.K.
LaGraff, J.E., Syracuse University, Syracuse, N.Y., U.S.A.
Ashworth, D.A., Rolls-Royce, plc., Bristol, U.K.
Jones, T.V., Oxford University, Oxford, U.K.

Measurements have been made of instantaneous heat transfer rates to a surface under a transitional boundary layer. The thin film surface heat transfer instrumentation used in the study was capable of time resolving the effects of changes in heat transfer within an accuracy of 10 µsecs. The tests were conducted in the Oxford University 6 inch Isentropic Light Piston Tunnel (ILPT) under simulated gas turbine Reynolds numbers, Mach numbers, and gas-to-wall temperature ratios.

The ability to observe and track the end stage of the transition process (i.e. turbulent spots) in a laminar boundary layer undergoing transition (see Figure 1) allowed turbulent spot generation rates, convection speeds, and spreading angles to be estimated. The important fluid dynamic parameters of Mach number, Reynolds number, pressure gradient, and freestream turbulence intensity were varied independently in these tests.

Using quantitative values of the measured turbulent spot characteristics, a simple time marching code was developed based on Emmons' turbulent spot theory to estimate the intermittency. This work was sponsored by AFOSR under grant number 89-0427.

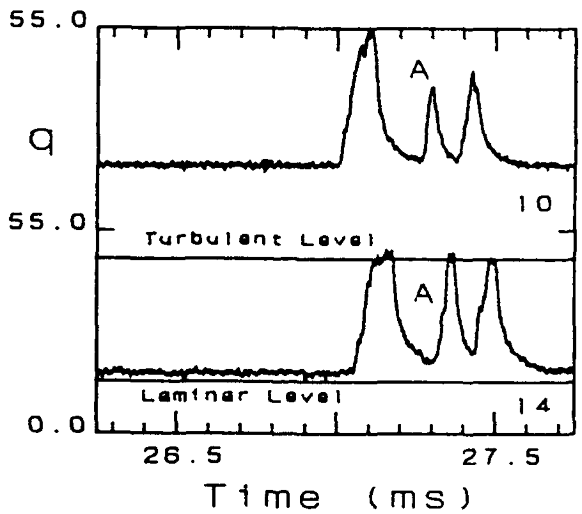

Figure 1 - Expanded scale heat transfer traces (q in kW/m²). Re_u=6x10⁶/m, T_O/T_W=1.4, Δx=8mm.